Guaiacol and its mixtures: new data and predictive models. Part 2: Gibbs energy of solvation

Mikhail A Varfolomeev, Ruslan N Nagrimanov, Mikhail A Stolov, Nicolas Ferrando, Rafael Lugo, Jean-Charles de Hemptinne

Guaiacol and its mixtures: new data and predictive models. Part 2: Gibbs energy of solvation

Mikhail A. Varfolomeev[1], Ruslan N. Nagrimanov[1], Mikhail A. Stolov[1], Nicolas Ferrando[2], Rafael Lugo[2], Jean-Charles de Hemptinne[2]

[1]Department of Physical Chemistry, Kazan Federal University, Kremlevskaya str. 18, 420008 Kazan, Russia
[2]IFP Energies Nouvelles, 1-4 avenue de Bois-Préau 92852 Rueil-Malmaison, France

Abstract

Guaiacol is a model molecule for lignocellulosic biomass processing, and thus understanding its interactions with solvents is an important step when developing units for processing lignocellulosic biomass. In this work, activity coefficient measurements of different solvents (acetonitrile, ethanol, tetrahydrofuran) in guaiacol have been performed at different concentrations and temperatures. These measurements have been used to estimate the infinite dilution activity coefficients and the Gibbs energy of solvation of guaiacol in the different solvents, and of each solvent in guaiacol. These estimated values were compared to those obtained with different predictive models: UNIFAC DMD, Monte Carlo Molecular Simulation, COSMO-SAC and GC-PPC-SAFT. The predictions are in very good agreement with the Gibbs energies of solvation derived from experimental data. Some conclusions are also drawn regarding the inter and intramolecular hydrogen bonding in guaiacol and about its affinity with different solvents on the basis of the inter and intra molecular interactions taking place.

Keywords: activity coefficient; Gibbs energy of solvation; gas chromatography; GC-PPC-SAFT; Monte Carlo molecular simulation

---

1. Introduction

Lignocellulosic biomass (LCB) can be a potential resource for the production of different chemicalreagents and fuels. LCB usage will help to protect the environment and to reduce the dependence on fossil fuels, which is important for sustainable development of economics as well as for creation of new workplaces at the regional level and development of rural areas [1]. There is now a commitment from the chemical industry to develop new green chemistry-based processes [2-6], and LCB is called to play a major role as an alternative raw material. It has several advantages in comparison with fossil raw materials: renewable, widely available and better distributed throughout the world. Indeed, the lignocellulosic material can be used to obtain desired molecules for a certain applications, which are consistent with the principles of green chemistry [6]. However, the development of effective processes to

produce chemicals from LCB is limited by the availability of design tools that allow the prediction of physicochemical properties of molecules when one only knows their structure.

It is expected that bioresourceswill be processed in plants called biorefineries. As in classic refineries, biorefineriesconsist of unit operations where physics is governed by chemical thermodynamics. The design of green and innovative processes for the valorisation of biomass requires the understanding of the thermodynamic behaviour of species associated to LCB loads. These mixturesare particularly complex due to the wide variety of oxygenated compounds they might contain. In particular, the decomposition of the LCB raw material leads to the formation of a large variety of multifunctional oxygen-bearing compounds. This leads to strong polar and associating intra-and intermolecular interactions that make these mixtures highly non-ideal (from a thermodynamic point of view). The models used for hydrocarbons (models typically found in most process simulators) fail to reproduce these non-idealities.Therefore, the challenge for the design and optimization of biorefinery units is to have appropriate tools that can adequately reproduce the phase equilibrium and properties of thesemixtures, in the same way as fossil mixturesare described in current industrial applications.In addition, the context of European legislation (REACH) pushes the chemical industry to provide adequate predictive estimations of the possible effects of molecules on humans and the environment [7].

A good reproduction of phase equilibria is of special importance for the design of separation technologies in biorefineries.Predicting the affinity of oxygen-bearing molecules with respect to a given solvent is a relevant step for designing separation processes, and thus predictive models that are able to take into account the molecular diversity and the complex interactions taking place in biomass-based mixtures are required.

Guaiacolsare phenolic compounds that have a methoxy group and a hydroxyl group. Guaiacol and guaiacol derivatives are products of the breakdown of lignin when processing LCB. Guaiacols are used as model molecules to understand the breakdown of LCB [8-9]. Due to the presence of two oxygen-bearing groups and an aromatic ring, inter and intramolecular interactions play a major role in phase equilibrium and phase properties of pure guaiacoland its mixtures with polar and/or associating solvents. When inventorying the available phase equilibrium data for binary mixtures of guaiacol with different solvents[10], it appears that :

- The most frequent data in mixture with hydrocarbons (normal and *iso*-alkanes from C6 to C16) and some aromatics (benzene, toluene) are infinite dilution activity coefficients (IDAC) at two temperatures: 321 and 331 K. All these IDAC data are provided by the same author [10]. Notice that, due to the technological limitations

explained later in this paper, it is the IDAC of the solvent infinitely diluted in guaiacol that is provided.

- A few VLE / LLE data are provided for guaiacol with other solvents: water, some alcohols (methanol, ethanol and octanol) and benzene.

In the first part of this work devoted to guaiacol[11], the GC-PPC-SAFT EoS was used to reproduce the thermodynamic behavior of pure guaiacol and its mixtures with methane, carbon dioxide, ethanol, octanol, water, acetone, butyl acetate, *n*-hexadecane, hydrogen, carbon monoxide, hydrogen sulfide, ammonia. In particular, the choice of an appropriate association scheme for guaiacol was discussed. The importance of using binarymixtures data instead of pure compound data only was shown to be of major importance when dealing with such a choice.

In this work, we measured activity coefficients of binary mixtures of guaiacol with organic solvents at different composition of components and temperatures using the headspace method [12]. Headspace analysis became popular over recent years and has now gained worldwide acceptance for analyses of, for example, alcohols in blood and residual solvents in pharmaceutical products. It allows obtaining activity coefficients of solutesin a large range of concentration. Moreover, activity coefficients can be calculated for several solutes in multicomponent mixture simultaneously. However, there are some restrictions and limitations for this method. The most important for us is that the solute should have detectable saturated vapor pressure. Thus, activity coefficients of large molecules are analyzed with high uncertainties. Guaiacol has extremely low saturated vapor pressure and its vapor is barely appreciable by the detector of a gas chromatograph. Therefore activity coefficients of guaiacol are not measured in this work. They were obtained from the measured activity coefficients of solvents diluted in guaiacol, which were then used to fit the NRTL Gibbs energy model. The NRTL model was used to determine the guaiacol activity coefficient. This approach is consistent by virtue of the Gibbs-Duhem equation. The development and use of reliable predictive methods can resolve this restriction. The solvents used in this work were ethanol (EtOH), tetrahydrofuran(THF) and acetonitrile (ACN). From the measured activity coefficients, we deduced the infinite dilution activity coefficients (IDAC) using the correlative NRTL model to extrapolate the activity coefficients at infinite dilution conditions. The IDAC values were then converted into Gibbs energy of solvation and compared to the values predicted with different approaches, namely:

- Monte Carlo molecular simulation using the AUA force field and the thermodynamic integration technique [13].

- The group-contribution PPC-SAFT equation of state developed by Tamouza [14].
- The COSMO-SAC activity coefficient model [15-16].
- The UNIFAC PSRK model [17].

2. Experimental section

2.1 Materials

All samples used in this work were of commercial origin (see Table 1). Pure guaiacol (2-methoxyphenol) was purified by repeated vacuum fractional distillation under a nitrogen atmosphere. Acetonitrile, ethanol and tetrahydrofuranwere dried and purified before usage by standard methods [12] up to minimal mass fraction 0.995. Sample purities were determined by using the Agilent 7890 B gas chromatograph equipped with the flame ionization detector. The water content was determined by titration using Karl Fischer method.

Table 1

2.2 Head space analysis

Activity coefficients were obtained at 298.15 K for all investigated solutes and at 308.15 and 318.15 K for ethanol and THF. Measurements of activity coefficients were carried out by gas chromatographic headspace analysis technique using PerkinElmer Clarus 580 chromatograph with Turbomatrix HS-16 headspace autosampler. A detailed description of the experimental procedure was published elsewhere [12]. Equilibrium vapor phase samples were automatically taken from thermostated 22 ml vials containing 1-5 ml of solution or pure solute (volumes of solution and pure solute should be equal) and transferred to the gas chromatograph. Since the internal thermostat of the autosampler has a minimal temperature mode of 308.15 K, we used an external thermostat to perform measurements at 298.15 K.

The values of activity coefficients $\gamma^{A/S}$ (molecule A in solvent S) can be calculated from the ratio of vapor pressures of solute A over its solution in S and above pure A by equation (1):

$$\gamma^{A/S} = p^{A/S} / \left(p^{A}_{sat} \cdot x^{A/S} \right) \tag{1}$$

where $x^{A/S}$ is the molar fraction of A in solution. The ratio $p^{A/S} / p^{A}_{sat}$ is equal to the ratio of areas of chromatographic peaks in experiments with the solution and with pure A. In our calculations we made a correction of initial concentration of solute on the quantity of

evaporated solute in case of extremely low concentrations (in this situation we consider solution as infinitely diluted and the activity coefficient as a limiting activity coefficient). For higher concentrations of A we can neglect evaporation of solute. Measurements were carried out 5 times from each vial. An average value of $\gamma^{A/S}$was taken. Vapor pressure of solute can be calculated as$p^{A/S} = p_{sat}^{A} \gamma^{A/S} x^{A/S}$. Values of p_{sat}^{A} were taken from Dortmund Data Base [18]. Results are provided in Tables 2-4.

2.3 Exploitation of the experimental results with the NRTL model

As mentioned in the introductive section, the experimental setup and protocol used in this work to measure activity coefficients do not allow precisely measuring the activity coefficient of guaiacol dissolved in different solvents. This is due to the low volatility of guaiacol that leads to a vapor pressure which is poorlydetectable by the device used in our measurements. For this reason, in order to determine the activity coefficients of guaiacol and in order to extrapolate the available data towards infinite dilution conditions, we used the NRTL (Non-random Two-Liquid) activity coefficient model.

For each binary system guaiacol+solvent, the three NRTL parameters have been regressed (no temperature dependence was considered for the NRTL parameters since only data at 298.15 K were used in the regression). Model mean deviations on activity coefficients range between 1 and 3%.

3. Modeling and simulation

3.1 GC-PPC-SAFT EoS

The GC-PPC-SAFT (Group Contribution-Polar Perturbed-Chain Statistical Associating Fluid Theory) Equation of State is a predictive model based on the polar PC-SAFT equation developed by Gross and Sadowski[19-20], coupled to a group contribution method (GC). It is defined as a sum of Helmholtz energy contributions:

$$A^{res} = (mA^{hs} + A^{chain}) + A^{disp} + A^{assoc} + A^{multi-polar} \quad (2)$$

where the first four terms relate to the non-polar interactions and follow the theory developed by Gross and Sadowski[19-20], the last incorporate the contribution of polar interactions[21]. The reader can refer to the original papers for a more detailed description of this equation. In

3.1.1 and 3.1.2 we provide a detailed description of the pure compounds and mixtures parameters and the way they were obtained using the group contribution approach.

3.1.1 Purecomponents parameters

In GC-PPC-SAFT, the segment parameters (ε and σ) and the chain parameter m of the molecule are calculated from group contribution parameters ε_k, σ_k and R_k using the following relations inspired by the Lorentz-Berthelot combining rules:

$$\varepsilon = \sum_{k=1}^{n_{groups}} n_i \sqrt{\left(\prod_{k=1}^{n_{groups}} \varepsilon_k^{n_k} \right)} \quad (3)$$

$$\sigma = \sum_{k=1}^{n_{groups}} n_k \sigma_k \Big/ \sum_{i=1}^{n_{groups}} n_k \quad (4)$$

$$m = \sum_{k=1}^{n_{groups}} n_k R_k \quad (5)$$

wheren_k is the number of groups *k* in the molecule made of n_{groups} different groups.

For polar compounds, additional parameters are required: for dipolar compounds (water, alkanols), the dipole moment μ and dipole fraction $\left(x_p^{\mu}.m\right)$, and for quadrupolar compounds (aromatic hydrocarbons), the quadrupole moment Q and its corresponding quadrupolar fraction $\left(x_p^{Q}.m\right)$. These parameters are only relevant to polar and quadrupolar groups.

Finally, association interactions are considered using a specific term. This association term requires other specific parameters: association scheme and self-association energy (ε^{AB}) and volume (κ^{AB}). Self-association parameters are required for water and alkanols, and more generally, for all molecules containing associative molecular groups (e.g. hydroxyl groups).

In previous works, all pure compound parameters for small molecules as well as group parameters for hydrocarbons and most oxygen-bearing molecules have been determined [11,21].

In this work, we have used the group-contribution description of guaiacol proposed by Gambini*et al* [11] for the GC-PPC-SAFT model. The corresponding group parameters, taken from [11] can be found in Table 5. Gambini*et al*[11] proposed two sets of parameters depending on the number of associative sites considered in the guaiacol molecule. In this work, on the basis of results obtained by Gambini*et al* [11], we considered scheme presented

on Fig. 1. According to this scheme molecule of guaiacol forms intramolecular hydrogen bond. Existence of this interaction was supported previously by experimental studies [22]. The enthalpy of formation of intramolecular hydrogen bond in guaiacol is equal to – 13.5÷ -14.3 kJ mol^{-1}.

Table 5

Figure 1

For pure solvents, the following parameterization was used:

- Ethanol: a group-contribution description of ethanol was used. The group parameters were taken from previous works [21] and are provided in Table 5.

- Acetonitrile (ACN) and tetrahydrofuran (THF): no group contribution approach was applied for these molecules, for which molecular parameters were determined instead. These molecules have been considered aspolar andnonself-associating compounds (cross association is allowed). The dispersive, repulsive, chain parameters and the dipole fraction were simultaneously regressed on vapor pressure, liquid molar volume and infinite dilution activity coefficient in mixtures of these compounds with *n*-hexane. The association parameters (for cross-association phenomena) were then regressed using the available VLE data for mixtures of these compounds with associating molecules such as alcohols (propanol for ACN) or phenols (phenol for THF). The group parameters used for describing alcohols and phenols for solvent parameterization purposes are provided in Table 5. The deviations on vapor pressure and saturated liquid molar volume of pure ACN and THF as well as deviations on binary mixtures data are given in Tables 7-9. The resulting parameters for pure ACN and THF are provided in Table 6.

Table 6

Table 7

Table 8

Table 9

3.1.2. Mixture parameters

For mixtures containing compounds of different structures and polarities, combining rules must be defined. To improve the reproduction of phase equilibrium data, two interaction parameters could be considered: dispersive binary interactions parameters and cross-association parameters. Nevertheless, in order to check the predictability of the models, binary parameters were not taken into account in this work.

3.2 COSMO-SAC activity coefficient model

The COSMO (Conductor-like Screeening Model) family models allow computation of excess Gibbs energy in a fully predictive manner through an activity coefficient model. Several versions of COSMO have been developed in the past. Variants of the COSMO model such as the COSMO-SAC [15] and the COSMO-RS(Ol) [24] models have been proposed and refined in the last ten years. The COSMO-SAC model has been used in this work. It has proven to be quite reliable in predicting phase equilibria of binary mixtures from a qualitative point of view, although some improvements have been achieved in the subsequent years of its original publication for hydrogen bonding systems and liquid-liquid equilibria (LLE).

The first step of COSMO method is an *ab initio* DFT/COSMO calculation which determines the screening charges on a discretised cavity surrounding of molecule. These charges provide the so-called sigma profile (probability of finding a surface segment with a certain screening charge density).For mixtures, a weighted average contribution of each component is considered.

The second step is to calculate activity coefficients of the segments which lead to the activity coefficient of the solute by summation of segments contributions and addition of a combinatorial term (see original papers for more details[15,24]).

In this work we have used the modified version of Mullins *et al* [15] of COSMO-SAC combined with the VT-2005 database of sigma profiles [16].

3.3 UNIFAC Dortmund model

The group contribution method UNIFAC (UNIQUAC Functional Group ActivityCoefficients) published in the 70’s andfurther improved inits Dortmund version[25] was used to predict the required activity coefficients of the systems investigated in this paper. The reader can refer to the original papers for a more detailed description of the model and its parameters.It should be noticed that the modified UNIFAC (Dortmund) model is widely recognized in industry as one of the best UNIFAC versions for predicting activity coefficients in industrial applications. This model is currently available in most process simulators. In this work, published parameters as well as some parameters delivered by the UNIFAC consortium to its members were used.

3.4 Molecular simulation

For many years, molecular simulation has been successfully used to predict phase equilibrium and thermophysical properties of systems of industrial interest [13,26]. Various simulation techniques are devoted to the prediction of solvation energies, such as free energy perturbation [27], thermodynamic integration [28], slow-growth method [29] or umbrella sampling [30]. The thermodynamic integration technique will be used in this work in association with Monte Carlo simulations. The solvation free energy ΔG^{solv} is defined by the free energydifference given by the total reversible work associated withchanging the Hamiltonian of the system from the gas (vacuum)to the liquid phase [31]. As free energy is a state function, it can be calculated from a thermodynamic cycle including non-physical transformations, as shown in Fig.2.

Figure 2

Following this cycle, the solvation free energy is given by:

$$\Delta G^{solv} = \Delta G^{solv}_{VdW} + \Delta G^{solv}_{elec} + \Delta G^{dummy} - \Delta G^{vacuum} \quad (6)$$

The terms ΔG^{solv}_{VdW} and ΔG^{solv}_{elec} correspond to the free energy of "insertion" of the bonded assembly of uncharged Lennard-Jones spheres and to the free energy required for "charging" the solute[32].The term ΔG^{vacuum} corresponds to the same transformation, but in vacuum instead of solvent. It is therefore only related to the intramolecular dispersion-repulsion and electrostatic energy of the solute.In this work, we assume that this contribution can be neglected (which is indeed the case for solute molecules modeled by rigid force fields). Finally, the term ΔG^{dummy} is the solvation free energy of a non-interacting particle (that is, a particle without intermolecular van der Waals or electrostatic interactions energies, but with the same intramolecular energy asthe solute), and is equal to zero. The thermodynamic integration method consists in evaluating a free energy difference using the following expression:

$$\Delta G = \int_0^1 \left\langle \frac{\partial U(\lambda)}{\partial \lambda} \right\rangle d\lambda \quad (7)$$

where U is the interaction potential between solute and solvent, and $\lambda$is a coupling variable: $\lambda = 1$ means a full coupling between the solute and the solvent molecules, while $\lambda = 0$ means that solute does not interact with the solvent. To avoid molecule overlapping for low values of λ, a soft-core potential is used between a force center i of the solute and a force center j of a solvent molecule for dispersion-repulsion interactions [33]:

$$U_{ij}^{disp-rep} = 4\varepsilon_{ij}\lambda_{VdW}^{n}\left[\frac{1}{\left[\alpha\left(1-\lambda_{VdW}\right)^{2}+\left(\frac{r_{ij}}{\sigma_{ij}}\right)^{6}\right]^{2}}-\frac{1}{\alpha\left(1-\lambda_{VdW}\right)^{2}+\left(\frac{r_{ij}}{\sigma_{ij}}\right)^{6}}\right] \quad (8)$$

A value of 0.5 and 4 are used for α and n, respectively [31]. The electrostatic energy could be treated by a similar way, but the calculation of long range corrections becomes not obvious. Practically, the following coupling function can be used [32, 34, 35]:

$$U_{ij}^{elec} = \frac{\lambda_C q_i q_j}{4\pi\varepsilon_0 r_{ij}} \quad (9)$$

As a charge overlap could generate a singularity, the calculation of electrostatic energy for the various values of λ_C should be carried out for $\lambda_{VdW} = 1$ to ensure sufficient repulsion between atoms bearing electrostatic charges. The complete methodology can be summarized as follows:

- first, is calculated by fixing $\lambda_C = 0$ and by performing one Monte Carlo simulation per value of λVdW. The following 16 values of λ_{VdW} are selected: {0, 0.1, 0.2, 0.3, 0.35, 0.4, 0.425, 0.45, 0.475, 0.5, 0.55, 0.6, 0.7, 0.8, 0.9, 1}.
- second, is calculated by fixing $\lambda_{VdW} = 1$ and by performing one Monte Carlo simulation per value of λ_C. The following 11 values of λ_C are selected: {0, 0.1, 0.2, 0.3, 0.4, 0.5, 0.6, 0.7, 0.8, 0.9, 1}.
- third, is calculated by making variable λ_{VdW} and λ_C simultaneously with the following values {0, 0.1, 0.2, 0.3, 0.35, 0.4, 0.425, 0.45, 0.475, 0.5, 0.55, 0.6, 0.7, 0.8, 0.9, 1}

Except for the calculation of ΔG^{vacuum}, a Monte Carlo simulation consists in simulating a NPT ensemble at the desired temperature and pressure, with one molecule of solute, and a total of 500 molecules of solvent. When guaiacol is the solute (in this case, the solvent is ethanol or THF or ACN), a typical simulation run lasted for 150 million steps, including an equilibrium run of 80 million steps, a step corresponding to a single Monte Carlo move. When guaiacol is the solvent, the equilibrium step should be longer: a typical simulation run lasted

for 250 million steps, including an equilibrium run of 200 million steps. The different Monte Carlo moves and their corresponding attempt probabilities used during the simulations were molecular translation (30%), molecular rotation (30%), regrowth with configurational bias[27] (39.5%), and volume change (0.5%). In the case of Lennard-Jones interactions, a spherical cut-off equal to half of the simulation box was used while the classical tail correction was employed [13]. For long-range electrostatic energy, the Ewald summation technique was used with a number of reciprocal vectors k equal to 7 in all three space directions and a Gaussian width α_{red} equal to 2 in reduced units.

For the calculation of ΔG^{vacuum}, a Monte Carlo simulation consists in simulating a NPT ensemblecontaining only one solute molecule at the desired temperature and pressure. A simulation run lasted for 5 million Monte Carlo steps including an equilibrium run of 1 million MC steps, and only regrowth moves with configurational bias were carried out.

The force field used to simulate ethanol, guaiacol and tetrahydrofuranwas the AUA4 force field described in [11,37,38], respectively. For acetonitrile, the TraPPE-UA force field was used [39].

A typical <dU/dλ> versus λcurve is given in Fig. 3 for the example of solvation of guaiacol in acetonitrile. According to equation (7), these curves were integrated between 0 and 1 using the trapezoid method to obtain ΔG^{solv}.

Figure 3

4. Results and discussion

4.1 Activity coefficients

Figures 4-6 show measured in this work activity coefficients of ethanol, acetonitrile and tetrahydrofuranin mixture with guaiacol at different composition. Experimental activity coefficients are provided in Tables 2-4. These data are compared to the predictions provided by UNIFAC DMD, COSMO-SAC and GC-PPC-SAFT. Several points can be outlined from these results:

- The infinite dilution activity coefficients (IDAC) of ethanol and ACN are slightly larger than one, which means that, despite the possible cross association taking place between guaiacol and these molecules, their mutual affinity remains low at infinite dilution conditions. On the other hand, THF has a rather low IDAC in guaiacol,

meaning that cross association plays a major role in this system. According to work [22] THF forms stronger hydrogen bonds with methoxyphenols than ACN.

- Increasing of temperature induces increasing of activity coefficients values for ethanol and THF solutions in guaiacol.
- The UNIFAC DMD model leads to activity coefficients close to 1 for the whole composition range and for the three solvents considered in this work, i.e. the behavior predicted by UNIFAC DMD is almost ideal. This might be explained by the fact that the UNIFAC interaction parameters (residual term) between the group ACOH and the solvents THF or ACN are 0. In the case of the interactions between the groups ACOH and -OH, the parameters are different from 0 but the behavior remains close to ideal.
- The COSMO-SAC model leads systematically to low IDAC values, indicating that this model overestimates the cross association phenomenon for the binaries ethanol-guaiacol and ACN-guaiacol mixtures. On the other hand, this cross-association behavior is well confirmed by the experimental activity coefficients measured for THF-guaiacol.
- The GC-PPC-SAFT EoS leads to the best predictions for all the systems investigated in this work. Although some deviations are observed for the infinite dilution behavior. This model is able to qualitatively reproduce the expected physical behavior of the different solutions studied here. This is due to the fact that this model takes explicitly into account the different types of intermolecular interactions, and each interaction (e.g. association, dipole and quadrupole, etc.) is parameterized on the most relevant data.

Figure 4

Figure 5

Figure 6

4.2 Solvation Gibbs Energy

Infinite dilution activity coefficients (IDAC) are directly related to the Gibbs free energy of solvation of a solute in a given solvent. In this work, we used Monte Carlo molecular simulation to predict the Gibbs free energy of solvation of different solvents in guaiacol and of guaiacol in different solvents at 298.15 K. The simulations were carried out using the thermodynamic integration algorithm described in 3.4. The results obtained are

shown in Table 10. The Gibbs free energies of solvation of these systems were also predicted using the GC-PPC-SAFT EoS. Predictions were also made using the COSMO-SAC and the UNIFAC DMD models.

Table 10

In order to compare these predictions with the experimental data obtained in this work, IDAC were determined by fitting the available activity coefficient data using the NRTL model. In this way, the IDAC of ethanol, THF or ACN in guaiacol at 298.15 K were obtained. The corresponding IDAC values were obtained with the NRTL model, fitted on the activity coefficients of solvents in guaiacol. It is known that, due to the Gibbs-Duhem relation, this procedure is consistent.

The conversion from IDAC to Gibbs energy of solvation $\Delta G_s^{A/B}$ was made using:

$$\Delta G_s^{A/B} = RTln\left(\frac{\gamma^{\infty,A/B} P^{\sigma,A}}{RT\rho_w^B}\right) \quad (11)$$

where A is the solute and B is the solvent, $\gamma^{\infty,A/B}$ is the IDAC of A in B, $P^{\sigma,A}$ is the vapor pressure of pure Aat T and ρ_w^B is the molar density of the solvent (in $molm^{-3}$).

Table 11 shows the values obtained for Gibbs energy of solvation from the fitted NRTL model (referred here as "experimental" values since they were deduced directly from the experimental data). In this table, the predicted Gibbs energies of solvation obtained using molecular simulation, GC-PPC-SAFT, COSMO-SAC and UNIFAC DMD are also shown.

Table 11

Before comparing the predicted results with the solvation energies derived from the experimental data, notice that Table 10 shows that the electrostatic interaction is in some cases the most important component of the total Gibbs energy of solvation. At the same time, the absolute values of the statistical uncertainty associated to the Gibbs energies of solvation predicted by MS are rather low.

As shown in Table 11, all the models predict negative solvation energies meaning that the solute-solvent affinity is well reproduced by all models. The models were also able to reproduce the relative differences in terms of solvation energies between the systems investigated in this work. The results show that the mutual affinity of guaiacol and THF is superior to that of guaiacol with ACN or ethanol. The analysis of the results shows also that the best predictions are provided by the GC-PPC-SAFT model, with a mean absolute deviation of about ± 1$kJmol^{-1}$. Molecular Simulation using the thermodynamic integration algorithm and the force fields previously described gives an absolute deviation of about ± 4

kJ mol^{-1}, whereas this value is ± 3 kJ mol^{-1} for UNIFAC DMD. The highest deviations are observed for COSMO-SAC (the most predictive model) where the absolute deviations higher than ± 6 kJ mol^{-1}.

5. Conclusions

The activity coefficients of different solvents (tetrahydrofuran, acetonitrile and ethanol) in guaiacol have been measured by the head space technique. The detection limits of this technique depend on the volatility of the molecules being analyzed, and thus only the activity coefficients of volatile solvents in guaiacol could be measured. The infinite dilution activity coefficients (IDAC) of guaiacol in the solvent and that of the solvent in guaiacol could be obtained by fitting the NRTL model on the available experimental activity coefficients and then extrapolating it to infinite dilution conditions. The IDAC have then been converted into Gibbs energy of solvation. This experimentally derived Gibbs energy of solvation has been compared to the predictions using different models: UNIFAC DMD, COSMO-SAC, GC-PPC-SAFT and Monte Carlo molecular simulation with the AUA4 force field (except from ACN, for which the TraPPE UA force field was used). The results show that a good agreement is obtained between the predictions and the experimental derived values. The highest absolute deviations obtained are of the order of ± 6 kJ $mol^{-1}$and were observed for the COSMO-SAC model. The lowest deviations were obtained when applying the GC-PPC-SAFT model. The results show that the lowest Gibbs free energy of solvationis was obtained for guaiacol in THF due to stronger intermolecular hydrogen bonds, which is also consistent with the predictions.

Acknowledgements

This work has been partly performed according to the Russian Government Program of Competitive Growth of Kazan Federal University. R.N. gratefully acknowledges the financial support by the research grant of Kazan Federal University.

References

[1] J.C. Pasty, Les débouchés non alimentaires des produits agricoles : un enjeu pour la France et l'Union Européenne, Rapport du Conseil Economique et Social, 2004.

[2] T. Werpy, G. Petersen, Top value added chemicals from biomass. Volume I – Results of screening for potential candidates from sugars and synthesis gas, PNNL (DOE), 2004.
[3] J.E. Holladay, J.J. Bozell, J.F. White, D. Johnson, Top-value added chemicals from biomass. Volume II–Results of screening for potential candidates from biorefinery lignin,PNNL(DOE), 2007.
[4] P. Desmarescaux, Situation et perspectives de developpement des productions agricoles a usage non alimentaire, Rapport Ministère de l'Agriculture et de la Pêche, 1998.
[5] D.R. Dodds, R.A. Gross, Chemicals from biomass,Science 318 (2007) 1250-1251.
[6] Gallezot P. Chapter 3: Process options for the catalytic conversion of renewables into bioproducts, In: Catalysis of renewables. Wiley Interscience, 2007.
[7] C. Nieto-Draghi, G. Fayet, B. Creton, X. Rozanska, P. Rotureau, J.C.de Hemptinne, Ph. Ungerer, B. Rousseau, C. Adamo, A general guidebook for the theoretical prediction of physicochemical properties of chemicals for regulatory purposes,Chem. Rev.115(2015) 13093–13164.
[8] Q. Lu, W.Z. Li, X.F. Zhu, Overview of fuel properties of biomass fast pyrolysis oils, Energy Convers. Manage.50 (2009) 1376–1383.
[9] A. Oasmaa, E. Kuoppala, Solvent fractionation method with brix for rapid characterization of wood fast pyrolysis liquids, Energy Fuels 22 (2008) 4245–4248.
[10] DETHERM: Thermophysical Properties of Pure Substances and Mixtures, version 2012, DECHEMA, Frankfurt am Main, 2012.
[11] C.G. Pereira, C.Féjean, S.Betoulle, N. Ferrando, R. Lugo, J.C. Hemptinne, P.Mougin, Guaiacol and its mixtures: new data and predictive models Part 1:Phase equilibrium,Fluid Phase Equilib. (2017) submitted FPE-S-17-00725
[12] N.H.Snow, G.C. Slack, Head-space analysis in modern gas chromatography,Trends Anal. Chem. 21 (2002) 608-617.
[13] P. Ungerer, B. Tavitian, A. Boutin, Applications of molecular simulation in the oil and gas industry, 1st ed., Editions Technip, 2005.
[14] S. Tamouza, J.P. Passarello, P. Tobaly, J.C. de Hemptinne, Group contribution method with SAFT EOS applied to vapor liquid equilibria of various hydrocarbon series,Fluid Phase Equilib. 222-223 (2004) 67-76.
[15] S.T. Lin, S.I. Sandler, A priori phase equilibrium prediction from a segment contribution solvation model, Ind. Eng. Chem. Res. 41 (2002)899-913.

[16] E. Mullins, R.Oldland, Y.A. Liu, Sh. Wang, S.I. Sandler, C.-C. Chen, M.Zwolak, K.Seavey, Sigma-profile database for using cosmo-based thermodynamic methods, Ind. Eng. Chem. Res. 45(2006) 3973-3999.

[17] T. Holderbaum, J. Gmehling, A group contribution equation of state based on UNIFAC,Fluid Phase Equilib.70 (1991)251-265.

[18] http://ddbonline.ddbst.de/AntoineCalculation/AntoineCalculationCGI.exe

[19] J. Gross, G.Sadowski, Application of perturbation theory to a hard-chain reference fluid: an equation of state for square-well chains, Fluid Phase Equilib. 168 (2000) 183-199.

[20] J.Gross, G. Sadowski, Perturbed-Chain SAFT: An equation of state based on a perturbation theory for chain molecules,Ind. Eng. Chem. Res. 40 (2001) 1244-1260.

[21] D.Nguyen-Huynh, J.P.Passarello, P.Tobaly, J.C. de Hemptinne, Application of GC-SAFT EOS to polar systems using a segment approach,Fluid Phase Equilib. 264 (2008) 62-75.

[22] M.A. Varfolomeev, D.I. Abaidullina, B.N. Solomonov, S.P. Verevkin, V.N.Emel'yanenko, Pairwise substitution effects, inter- and intramolecular hydrogen bonds inmethoxyphenols and dimethoxybenzenes. thermochemistry, calorimetry, andfirst-principles calculations, J. Phys. Chem. B 114 (2010) 16503–16516.

[23] J.R. Rowley, W.V. Wilding, J.L. Oscarson, N.F. Giles, DIPPR data compilation of pure chemical properties; design institute for physical properties, AIChE: New York, NY, 2011.

[24] A.Klamt, COSMO-RS: From quantum chemistry to fluid phase thermodynamics and drug design, Elsevier, Amsterdam, 2005.

[25] J.Lohmann, R.Joh, J.Gmehling, From UNIFAC to Modified UNIFAC (Dortmund). IECR 40 (2001) 957–964.

[26] D.N. Theodorou, Progress and outlook in Monte Carlo simulations, Ind. Eng. Chem. Res. 49 (2010) 3047–3058.

[27] D.Frenkel, B.Smit, Understanding molecular simulation: from algorithms to applications, Academic Press, San Diego, CA, 1996.

[28] R. W.Zwanzig, High-temperature equation of state by a perturbation method. I. Nonpolar gases,J. Chem. Phys. 22 (1954) 1420−1426.

[29] I.Nezbeda, J. Kolafa, A new version of the insertion particle method for determining the chemical potential by Monte Carlo simulation, Mol. Simul. 5 (1991) 391−403.

[30] G.M.Torrie, J.P.Valleau, Nonphysical sampling distributions in Monte Carlo free-energy estimation: Umbrella sampling,J. Comput. Phys. 23 (1977) 187−199.

[31] C. Chipot, A. Pohorille, Free Energy Calculations, Springer Series in Chemical Physics, Springer, 2007.

[32] M.R. Shirts, J.W. Pitera, W.C. Swope, V.S. Pande, Extremely precise free energy calculations of amino acid chain analogs: comparison of common molecular mechanics force fields for proteins, J. Chem. Phys. 119 (2003) 5740−5761.

[33] T.C.Beutler, A.E. Mark, R.C.Vanschaik, P.R.Gerber, W.F. Vangunsteren, Avoiding singularities and numerical instabilities in free energy calculations based on molecular simulations,Chem. Phys. Lett. 222 (1994) 529-539.

[34] N.M. Garrido, M.Jorge, A.J. Queimada, I.G. Economou, E.A. Macedo, Molecular simulation of the hydration gibbs energy of barbiturates, Fluid Phase Equilib.289 (2010) 148-155.

[35] N. Ferrando, I.Gedik, V. Lachet, L.Pigeon, R.Lugo, Prediction of phase equilibrium and hydration free energy of carboxylic acids by Monte Carlo simulations, J. Phys. Chem. B 117 (2013) 7123-7132.

[36] M.P. Allen, D.J. Tildesley, Computer simulation of liquids, Oxford University Press, New-York, 1987.

[37] N. Ferrando, V. Lachet, J.M. Teuler, A. Boutin, Transferable force field for alcohols and polyalcohols, J. Phys. Chem. B 113 (2009) 5985-5995.

[38] N. Ferrando, V. Lachet, J. Perez-Pellitero, A.D. Mackie, P. Malfreyt, A. Boutin, A transferable force field to predict phase equilibria and surface tension of ethers and glycol ethers, J. Phys. Chem.B115 (2011) 10654-10664.

[39] C.D.Wick, J.M.Stubbs, N.Rai, J.I. Siepmann, Transferable potentials for phase equilibria. 7. primary, secondary, and tertiary amines, nitroalkanes and nitrobenzene, nitriles, amides, pyridine, and pyrimidine,J. Phys. Chem. B109 (2005) 18974-18982.

Table 1

Origin, purity, method of purification and analysis of samples.

Table 2

Activity coefficients and vapor pressures of acetonitrile (A) in guaiacol at 298.15 K and different composition of the mixture.

Table 3

Activity coefficients and vapor pressures of tetrahydrofuran (A) in guaiacolat three temperatures (298.15 K, 308.15 K and 318.15 K) and different composition of the mixture.

Table 4

Activity coefficients and vapor pressures of ethanol (A) in guaiacolat three temperatures (298.15 K, 308.15 K and 318.15 K) and different composition of the mixture.

Table 5

Group parameters of GC-PPC-SAFT Equation of State from [11].

Table 6

Parameters of GC-PPC-SAFT Equation of State for acetonitrile (ACN) and tetrahydrofuran (THF).

Table 7

Standard deviations for vapor pressure and saturated liquid molar volume of acetonitrile and tetrahydrofuran (279-495 K) (pure component data were taken from [22]).

Table 8

Standard deviations for the VLE and IDAC data used for regressing the PPC-SAFT parameters of pure acetonitrile (ACN).

Table 9

Standard deviations for the VLE and IDAC data used for regressing the PPC-SAFT parameters of pure tetrahydrofuran (THF).

Table 10

Gibbs free energy of solvation predicted by molecular simulation at 298.15 K.

Table 11

Gibbs free energy of solvation of the binary system guaiacol+solvent at 298.15 K obtained from the measured activity coefficients and comparison with the predictions by molecular simulation, GC-PPC-SAFT, COSMO-SAC and UNIFAC DMD.

Fig. 1. Schemeof association for guaiacol.

Fig. 2. Thermodynamic cycle for calculation of Gibbs free energy of solvation.

Fig. 3. Average derivatives of the van der Waals (top), electrostatic (middle) and intramolecular (down) energies with respect to λ in the case of solvation of guaiacol in acetonitrile.

Fig.4. Activity coefficient of ethanol (EtOH) in ethanol-guaiacol solutions at 298 K.

Fig.5. Activity coefficient of acetonitrile (ACN) acetonitrile-guaiacol solutions at 298K.

Fig.6. Activity coefficient of tetrahydrofuran (THF) in tetrahydrofuran-guaiacol solutions at 298K.

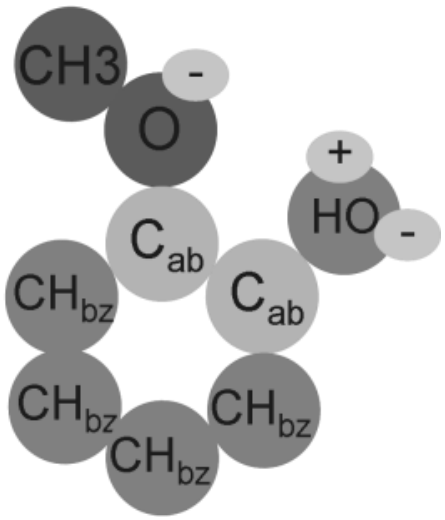

Fig.2. Schemeof association for guaiacol.

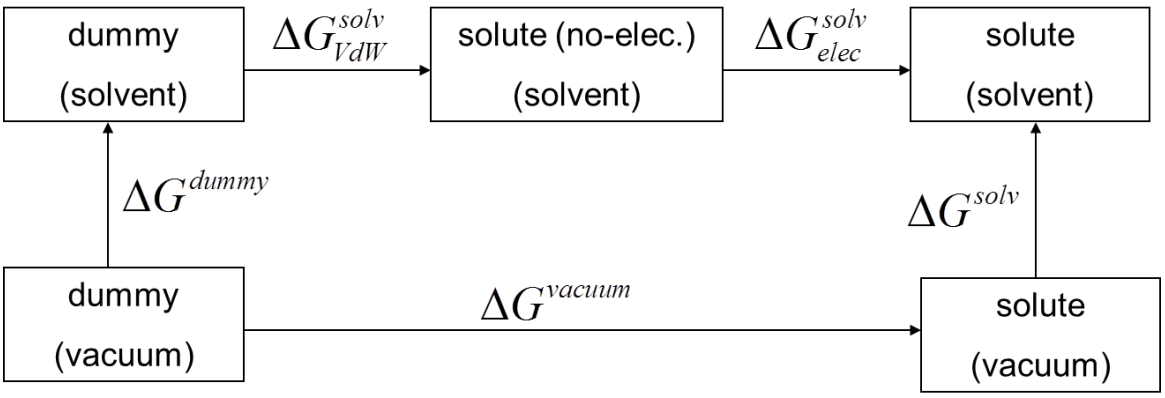

Fig. 2. Thermodynamic cycle for calculation of Gibbs free energy of solvation.

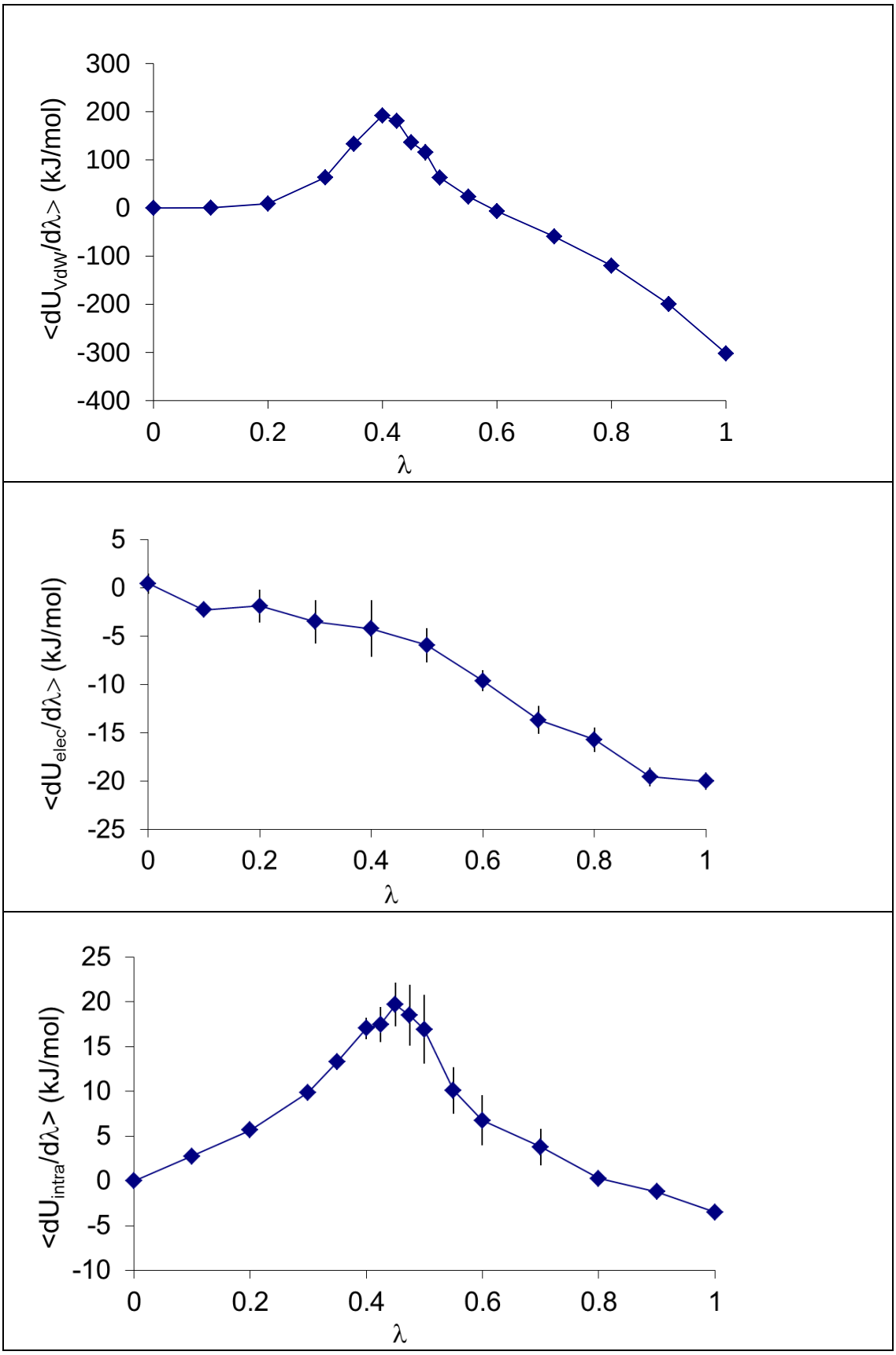

Fig. 3. Average derivatives of the van der Waals (top), electrostatic (middle) and intramolecular (down) energies with respect to λ in the case of solvation of guaiacol in acetonitrile.

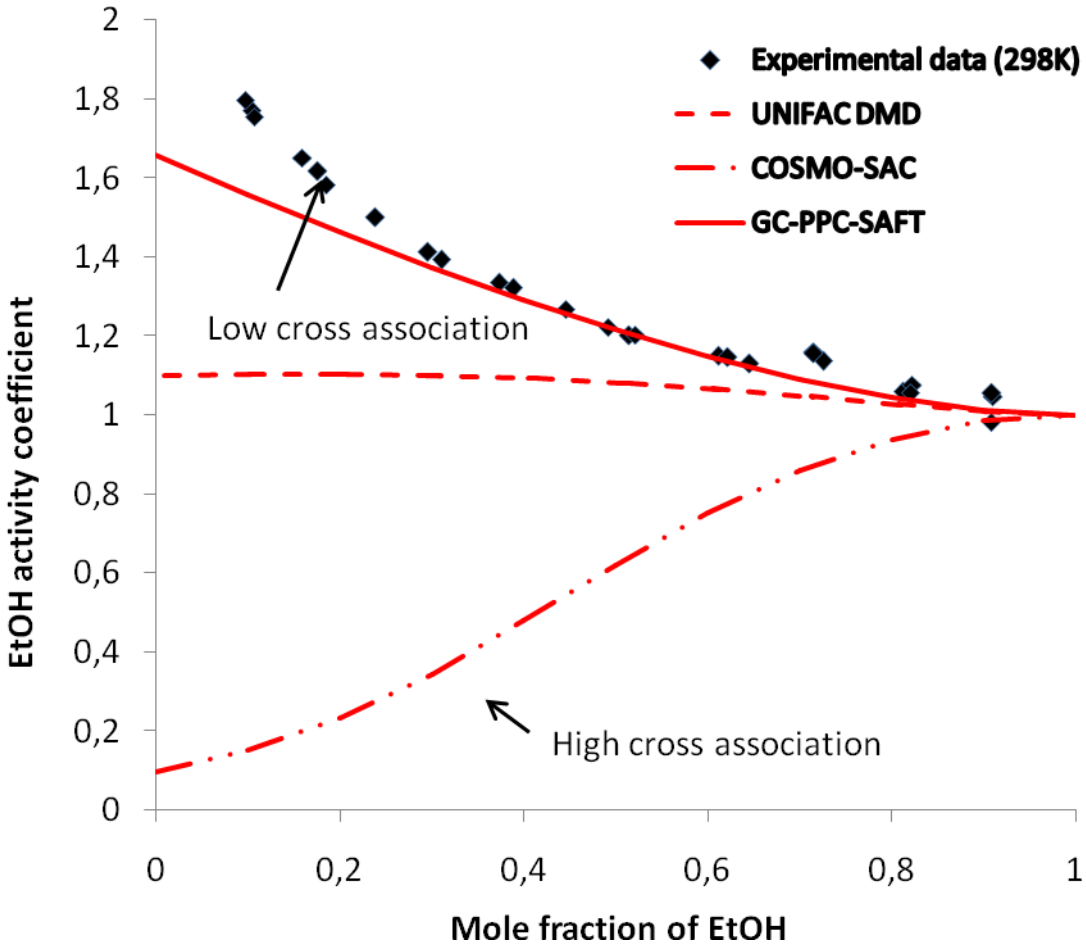

Fig.4. Activity coefficient of ethanol (EtOH) in ethanol-guaiacol solutions at 298K.

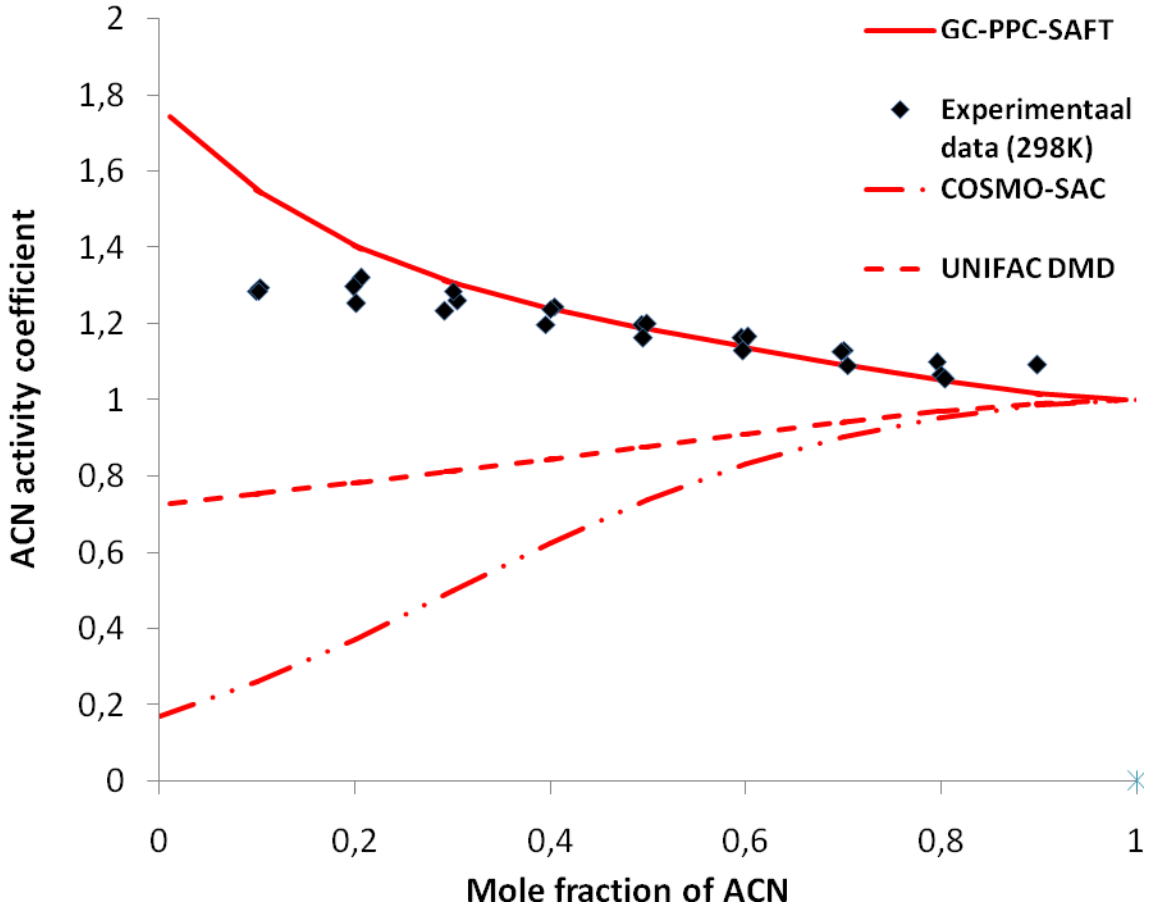

Fig.5. Activity coefficient of acetonitrile (ACN) acetonitrile-guaiacol solutions at 298K.

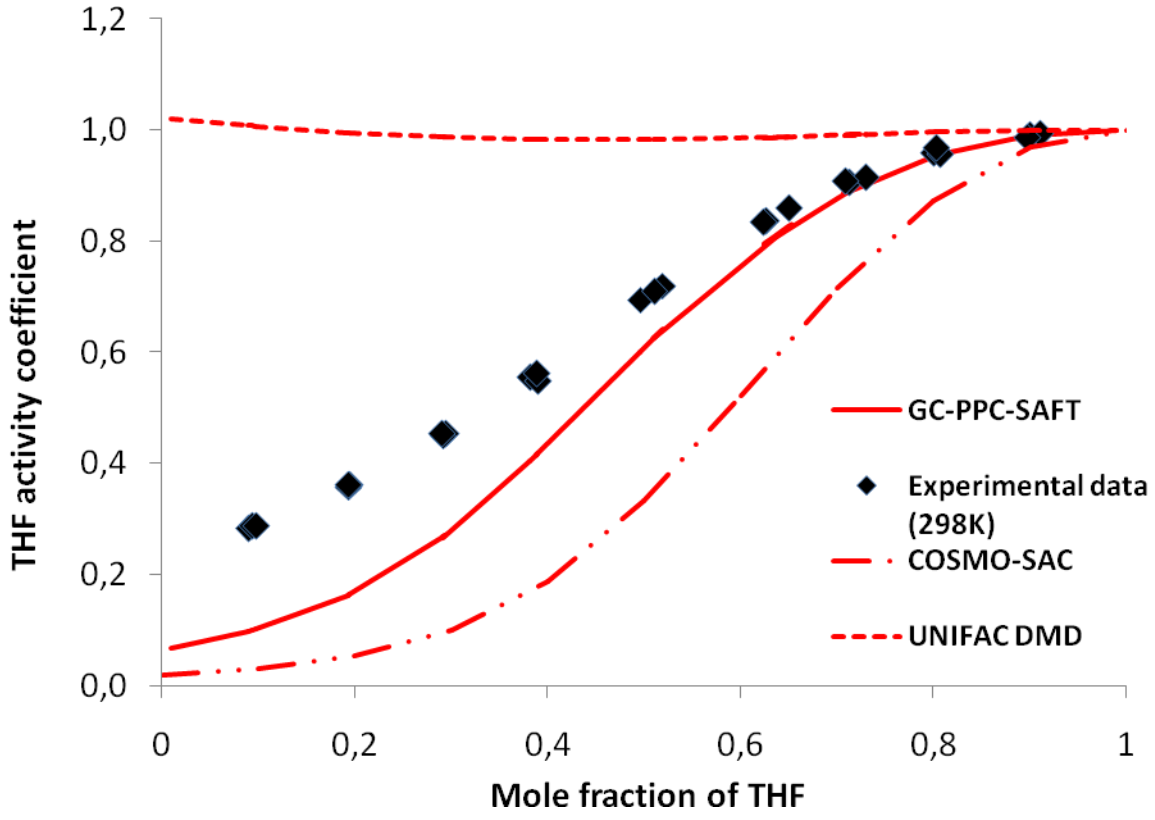

Fig.6. Activity coefficient of tetrahydrofuran (THF) in tetrahydrofuran-guaiacol solutions at 298K.

Table 1

Origin, purity, method of purification and analysis of samples.

Chemical Name	Source	Initial Mass Fraction Purity	Purification Method	Final Mass Fraction Purity	Analysis Method [a]	Mass faction of water
2-Methoxyphenol (guaiacol)	Aldrich	0.98	distillation	0.995	GC	0.0003
Acetonitrile	J.T. Baker	0.99	distillation	0.995	GC	0.0007
Ethanol	Spirtmed	0.95	distillation	0.995	GC	0.001
Tetrahydrofuran	BASF	0.98	distillation	0.999	GC	0.0002

[a] Gas chromatography.

Table 2

Activity coefficients and vapor pressures of acetonitrile (A) in guaiacol at 298.15 K and different composition of the mixture.

x^A	$\gamma^{A/Gua}$	P^A / kPa
0.1036	1.295	1589
0.0989	1.297	1519
0.1011	1.286	1539
0.2062	1.286	3139
0.1983	1.321	3101
0.2012	1.297	3089
0.3048	1.254	4526
0.3005	1.262	4489
0.2919	1.286	4442
0.4045	1.234	5908
0.4000	1.245	5897
0.3956	1.239	5805
0.4932	1.198	6995
0.4988	1.196	7063
0.4948	1.199	7026
0.5959	1.163	8205
0.6021	1.163	8293
0.5976	1.167	8253
0.7011	1.129	9371
0.6985	1.131	9352
0.7049	1.128	9415
0.7957	1.092	10285
0.8002	1.100	10425
0.8984	1.068	11356
0.9013	1.056	11264
0.8973	1.092	11605

Table 3

Activity coefficients and vapor pressures of tetrahydrofuran (A) in guaiacol at three temperatures (298.15 K, 308.15 K and 318.15 K) and different composition of the mixture.

T/K = 298.15			T/K = 308.15			T/K = 318.15		
x^A	$\gamma^{A/Gua}$	P^A / *kPa*	x^A	$\gamma^{A/Gua}$	P^A / *kPa*	x^A	$\gamma^{A/Gua}$	P^A / *kPa*
0.0895	0.283	546	0.1010	0.348	1155	0.0947	0.373	1720
0.0938	0.287	580	0.0980	0.347	1115	0.0978	0.379	1806
0.0979	0.287	607	0.1005	0.344	1136	0.0812	0.369	1461
0.1932	0.358	1493	0.1918	0.420	2642	0.1923	0.438	4104
0.1946	0.360	1515	0.1955	0.426	2731	0.1939	0.436	4121
0.1939	0.362	1514	0.1966	0.415	2677	0.1907	0.433	4024
0.2940	0.453	2878	0.2944	0.496	4795	0.2930	0.502	7166
0.2911	0.450	2829	0.3013	0.505	4995	0.2922	0.508	7235
0.2905	0.453	2843	0.2935	0.496	4778	0.2914	0.513	7279
0.3818	0.554	4569	0.3952	0.597	7738	0.3767	0.587	10782
0.3899	0.548	4612	0.3846	0.589	7440	0.3905	0.600	11410
0.3886	0.561	4713	0.3829	0.591	7428	0.3843	0.596	11149
0.4958	0.694	7437	0.4720	0.685	10606	0.4863	0.701	16618
0.5193	0.720	8073	0.4830	0.692	10966	0.4939	0.714	17182
0.5103	0.710	7830	0.4941	0.706	11458	0.4939	0.711	17107
0.6503	0.859	12068	0.6132	0.824	16582	0.5980	0.802	23379
0.6266	0.836	11312	0.6043	0.816	16196	0.5895	0.782	22458
0.6240	0.835	11250	0.6086	0.819	16365	0.6001	0.808	23624
0.7131	0.906	13959	0.6966	0.888	20311	0.6888	0.873	29297
0.7306	0.915	14435	0.7051	0.898	20792	0.7050	0.884	30350
0.7087	0.907	13890	0.7167	0.894	21024	0.7028	0.881	30165
0.8006	0.958	16562	0.7946	0.946	24673	0.7979	0.935	36351
0.8069	0.956	16658	0.7962	0.948	24774	0.8003	0.942	36715
0.8035	0.967	16785	0.7983	0.949	24867	0.7919	0.930	35884
0.8994	0.991	19247	0.8529	0.977	27366	0.8938	0.980	42682
0.9108	0.993	19531	0.8891	0.980	28588	0.8907	0.970	42092
0.8979	0.987	19140	0.8935	0.984	28853	0.9005	0.975	42792

Table 4

Activity coefficients and vapor pressures of ethanol (A) in guaiacol at three temperatures (298.15 K, 308.15 K and 318.15 K) and different composition of the mixture.

T/K = 298.15			T/K = 308.15			T/K = 318.15		
x^A	$\gamma^{A/Gua}$	P^A / *kPa*	x^A	$\gamma^{A/Gua}$	P^A / *kPa*	x^A	$\gamma^{A/Gua}$	P^A / *kPa*
0.1046	1.771	1464	0.1035	1.691	2396	0.1037	1.745	4158
0.1074	1.755	1491	0.1046	1.678	2404	0.1056	1.704	4136
0.0974	1.797	1384	0.1019	1.685	2350	0.1063	1.701	4156
0.1594	1.651	2081	0.1925	1.523	4015	0.1841	1.567	6631
0.1758	1.617	2246	0.2082	1.482	4223	0.1852	1.553	6610
0.1854	1.583	2320	0.2066	1.496	4234	0.2106	1.525	7384
0.2961	1.412	3305	0.3118	1.344	5739	0.3131	1.378	9916
0.3105	1.394	3421	0.2940	1.370	5517	0.2995	1.354	9319
0.2387	1.500	2831	0.4052	1.248	6925	0.2709	1.428	8894
0.4457	1.267	4465	0.4055	1.253	6955	0.4169	1.266	12135
0.3734	1.335	3942	0.4145	1.237	7020	0.4246	1.260	12299
0.3887	1.322	4063	0.5073	1.183	8220	0.4235	1.263	12290
0.4918	1.223	4754	0.5038	1.180	8141	0.5108	1.226	14392
0.5145	1.202	4888	0.5160	1.174	8293	0.5152	1.218	14421
0.5214	1.202	4957	0.6137	1.118	9397	0.5096	1.225	14347
0.6117	1.150	5560	0.6115	1.121	9391	0.6111	1.156	16236
0.6220	1.146	5635	0.6057	1.125	9330	0.6073	1.160	16193
0.6456	1.129	5765	0.7138	1.066	10423	0.6066	1.163	16213
0.7254	1.136	6516	0.7129	1.078	10521	0.7125	1.106	18105
0.7153	1.160	6563	0.8092	1.039	11510	0.7048	1.105	17900
0.7149	1.157	6537	0.8110	1.036	11503	0.7154	1.103	18131
0.8118	1.058	6789	0.8078	1.038	11475	0.8081	1.061	19703
0.8229	1.077	7003	0.9048	1.008	12492	0.8018	1.065	19633
0.8203	1.057	6855	0.9030	1.010	12487	0.8015	1.041	19170
0.9081	0.981	7046	0.9013	1.007	12424	0.8975	1.031	21263
0.9103	1.046	7532				0.8885	1.028	21004
0.9088	1.056	7584						

Table 5

Group parameters of GC-PPC-SAFT Equation of State from [11].

Group	***ε/k (K)***	***σ (Å)***	***μ (D)***	$x_p^{\mu}m$	***Q (B)***	$x_p^{Q}m$	n_{sites}	***Charges***	***Associative Scheme***	ε^{AB}/k ***(K)***	κ^{AB}	R_1
(CH_3)	189.96	3.4873	-	-	-	-	-	-	-	-	-	0.7866
(CH_2)	261.09	3.9308	-	-	-	-	-	-	-	-	-	0.3821
$(C)_{AB}$	391.54	4.2783	-	-	-	-	-	-	-	-	-	0.00156
$(OH)_{\text{linear alcohols}}$	307.51	2.8138	1.7	0.5	-	-	3	-1 -1 +1	-	2143.3	0.00885	0.8318
$(OH)_{\text{phenol}}$	307.51	2.8138	1.2	0.5			3	-1 -1 +1	3B	1549.40	0.01985	1.0308
$(OH)_{\text{guaiacol}}$	307.51	2.8138	1.22	0.5	-	-	2	-1 +1	2B	812.17	0.2429	0.4040
$(O)_{\text{guaiacol}}$	280.96	3.5764	1.22	1.2	-	-	1	-1	-	2298.34	0.0051	0.4516
Phenol ring	-	-	-	-	7	0.25	1	-1	-	1000	0.01985	-
Guaiacol ring	-	-	-	-	8.5	0.25	0		-	0	0	-

Table 6

Parameters of GC-PPC-SAFT Equation of State for acetonitrile (ACN) and tetrahydrofuran (THF).

Group	***ε/k (K)***	***σ (Å)***	***m***	***μ (D)***	$x_p^{\mu}m$	n_{sites}	***Charges***	ε^{AB}/k ***(K)***	κ^{AB}
ACN	329.05	3.971	1.282	3.2999	0.678	2	-1 / -1	1007.6	0.05
THF	270.82	3.746	2.327	1.63	1.056	2	-1 / -1	2562.1	0.05

Table 7

Standard deviations for vapor pressure and saturated liquid molar volume of acetonitrile and tetrahydrofuran (279-495 K) (pure component data were taken from [23]).

	ACN	THF
Vapor pressure	1.5 %	1.9 %
Liquid volume	3.9 %	2.0 %

Table 8

Standard deviations for the VLE and IDAC data used for regressing the PPC-SAFT parameters of pure acetonitrile.

	VLE ACN + PrOH [10]	IDAC ACN in nC6 [10]
δP/P	1.7%	-
δy/y	2.8%	-
δIDAC/IDAC	-	12.5%

Table 9

Standard deviations for the VLE and IDAC data used for regressing the PPC-SAFT parameters of pure tetrahydrofuran (THF).

	VLE THF + PhOH [10]	IDAC THF in nC6 [10]
δ T	3.7 K	-
δy/y	0.63%	-
δIDAC/IDAC	-	4.72%

Table 10

Gibbs free energy of solvation predicted by molecular simulation at 298.15 K.

Solute	Solvent	dG VdW kJ mol^{-1}	dG Elec kJ mol^{-1}	dG intra kJ mol^{-1}[a]	**dG Solvation kJ mol^{-1}**	unc +/-
ACN	Guaiacol	2.44	-15.3	0	**-12.8**	0.5
THF	Guaiacol	-7.95	-5.4	0	**-13.4**	0.4
Ethanol	Guaiacol	-0.51	-13.8	0	**-14.3**	0.5
Guaiacol	ACN	-19.5	-8.6	6.0	**-34.2**	0.3
Guaiacol	THF	-25.5	-4.2	6.0	**-35.8**	0.4
Guaiacol	Ethanol	-21.8	-5.5	6.0	**-33.3**	0.7

[a] For ACN, THF and ethanol we assume that intramolecular interactions can be neglected.

Table 11

Gibbs free energy of solvation of the binary system guaiacol+solvent at 298.15 K obtained from the measured activity coefficients and comparison with the predictions by molecular simulation, GC-PPC-SAFT, COSMO-SAC and UNIFAC DMD.

ΔG_{solv} (kJ mol^{-1}) at 298.15 K						
Solute	Solvent	Exp (NRTL model)	MC MS	GC-PPC-SAFT	COSMO-SAC	UNIFAC - DMD
ACN	Guaiacol	-18.0	-12.8	-17.3	-23.1	-19.5
THF	Guaiacol	-21.3	-13.4	-24.0	-27.2	-17.2
Ethanol	Guaiacol	-18.0	-14.3	-18.4	-25.5	-19.5
Guaiacol	ACN	-33.5	-34.2	-35.0	-40.5	-38.6
Guaiacol	THF	-39.7	-35.8	-41.0	-46.2	-36.2
Guaiacol	Ethanol	-34.9	-33.3	-34.9	-41.7	-35.9